

## Synthesis and analysis of electrical properties of Lead free $Ba_3Sr_2LaTi_3V_7O_{30}$ Ceramics

P. S. Sahoo<sup>1</sup>, B. B. Mohanty<sup>1\*</sup>, J.Panda<sup>2</sup>, R. N. P. Choudhary<sup>3</sup>

<sup>1</sup>Department of Physics, Betnoti College Betnoti, Mayurbhanj, Orissa, India

<sup>2</sup>Department of Physics, BIET, Bhadrak, Orissa, India

<sup>3</sup>Department of Physics, ITER, Bhubaneswar, Orissa, India

---

**ABSTRACT:** Materials of tungsten-bronze (TB) structure belong to an important family of dielectric materials which are well known for their applications in various electrical devices, such as transducers, actuators, capacitors, and ferroelectric random access memory. The TB structure consists of a framework of distorted  $BO_6$  octahedral sharing corners in such a way that three different types of interstices (A, B and C) are available for a wide variety of cations occupying in a general formula  $(A_1)_2(A_2)_4(C)_4(B_1)_2(B_2)_8O_{30}$ . Our present work deals with the studies of preparation and characterization of the physical properties of a novel single-phase polycrystalline lead-free vanadate having Tungsten Bronze Structure with compound formula  $Ba_3Sr_2LaTi_3V_7O_{30}$ . The X-ray diffraction analysis confirms the formation of single-phase compound with orthorhombic structure. The effect of temperature (32- 500°C) and frequency ( $10^2$ – $10^6$  Hz) on structural and electrical properties were studied using an impedance analyzer. Detailed studies of impedance parameters provide a better understanding of the electrical properties and type of relaxation processes in the material. The bulk resistance is observed to be decreased with rise in temperature showing a typical negative temperature coefficient of resistance (NTCR) behavior.

**KEYWORDS:** TB Structure; Solid-state reaction; X-ray diffraction

---

### I. INTRODUCTION

Since the discovery of ferroelectricity in  $BaTiO_3$ , many ferroelectric compounds with tungsten-bronze structure have been widely investigated and found application particularly in devices such as transducers, actuators, capacitors, and nonvolatile ferro- electric random access memory because of their interesting ferroelectric, pyroelectric, piezoelectric, and nonlinear optic properties [1-5]. The TB structure consists of a complex array of distorted  $BO_6$  octahedra sharing corners in such a way that three different types of interstices (A, B and C) are available for cation occupying in the general formula  $(A_1)_2(A_2)_4(C)_4(B_1)_2(B_2)_8O_{30}$ . Generally, the smallest interstice C is empty, so the general formula is  $A_6B_{10}O_{30}$  for the filled tungsten-bronze structure. Nowadays, the research of lead-free electroce- ramics and their applications are extremely important as a result of implementing the strategy for the sustainable development of the world, and strengthening to the consciousness of environmental protection. Detailed litera- ture survey shows that though a lot of work has been done on TB structured compounds [6-11] but looking to the importance of the eco-friendly (lead-free) materials of the above family, we have recently carried out the systematic structural and electrical studies of the  $Ba_3Sr_2LaTi_3V_7O_{30}$  (BSLTV) compound.

### II. EXPERIMENTAL

The  $Ba_3Sr_2LaTi_3V_7O_{30}$  (BSLTV) ceramic has been synthesized by solid-state sintering method using high purity (>99.9%) precursors;  $BaCO_3$ ,  $SrCO_3$ ,  $La_2O_3$ ,  $TiO_2$ , (all from M/s Loba Chemicals Pvt. Ltd., Mumbai, India), and  $V_2O_5$  (M/s. Koch Light Ltd., England). The powders have been weighed in appropriate stoichiometric ratio and they were uniformly mixed in an agate mortar for 2h in an air atmosphere followed by wet methanol medium. Subsequently, it was calcined in an alumina crucible at 900°C for 12h. The calcined powders were re-grinded into very fine powders (with polyvinyl alcohol which was burnt out during sintering) and palletized into disks of 10 mm diameter and about 1-2 mm thickness using iso-static press at a pressure of  $4 \times 10^6$  N/m<sup>2</sup>. The pellets were then sintered at 950°C for 12 h in an air atmosphere using high limits alumina crucibles. Using X-ray diffraction (XRD) technique, the formation and quality of the compounds were checked. The X-ray diffraction patterns of the compounds was recorded at room temperature using an X-ray powder diffractometer (Rigaku, Miniflex) with  $CuK_\alpha$  radiation ( $1.5405\text{\AA}$ ) in a wide range of Bragg's angles  $2\theta$  ( $20^\circ \leq 2\theta \leq 80^\circ$ ) with a scanning rate of  $3^\circ$ / minute. The surface morphology of the sintered pellets was studied at room temperature by a scanning electron microscopy (SEM) (JEOL-JSM-5800). The electrical properties like

impedance and modulus studies and electrical conductivity ( $\sigma$ ) of the compounds were obtained as a function of frequency (10 kHz–1MHz) at different temperatures (32<sup>0</sup>C–500<sup>0</sup>C) using an impedance analyzer (PSM 1735, model:N 4L). The samples were preheated to 150<sup>0</sup> C for 4 h to remove the moisture if any. The hysteresis loops (P-E loop) of the poled samples (6 kV/cm for 36 h) were obtained using a workstation of hysteresis loop tracer (M/S Radiant Technology Inc, USA).

### III. RESULTS AND DISCUSSION

#### 3.1 Structural and microstructural studies

The room temperature XRD pattern of BSLTV are as shown in the Fig.1. The XRD pattern in the material is observed to be of different nature from that of the ingredient oxides, confirmed the formation of a single-phase new compound. The reflection peaks were indexed and the lattice parameters were determined in various crystal systems with cell configurations using computer software “POWDMULT” [11].

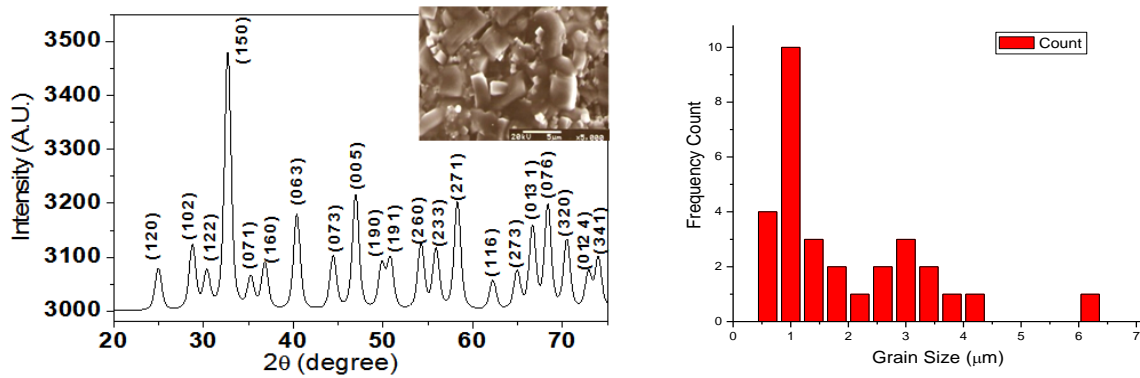


**Fig. 1. Room temperature XRD and SEM micrograph (inset) of  $\text{Ba}_3\text{Sr}_2\text{LaTi}_3\text{V}_7\text{O}_{30}$  and histograms (right) showing the grain size distribution**

A suitable unit cell (orthorhombic system) with lattice parameters:  $a=18.4411(27)$  Å,  $b=4.0456(27)$  Å,  $c=9.6524(27)$  Å (estimated standard deviations in parentheses) were chosen on the basis of the best agreement between observed (obs) and calculated (cal) interplaner distance  $d$  (i.e.,  $\sum (d_{\text{obs}} - d_{\text{cal}}) = \text{minimum}$ ).

The coherently scattered crystallite size of the sample was estimated from the broadening of the peaks ( $\beta_{1/2}$ ) using Scherrer’s equation [13];  $P=K\lambda/\beta_{1/2}\cos\theta_{hkl}$ , where  $K = \text{constant} = 0.89$ ,  $k = 1.5405$  Å and  $\beta_{1/2} = \text{peak width of the reflection at half height}$ . The average crystallite size of the compound was found to be 16 nm. The contributions of strain, instrumental and other unknown effects in the broadening have been ignored in the calculations. The SEM micrograph of the BSLTV compound at room temperature (Fig.1 (inset)) shows the homogenously and uniformly distributed grains over the entire surface of the sample. The average grain size evaluated from the histogram Fig. 1 (right) is found to be of 1.5 μm

#### 3.2. Impedance Properties

Complex impedance spectroscopy (CIS) [14] is a technique to characterize the electrical behavior of a system in which a number of strongly coupled processes exist. It helps to separate grain (intragrain) and grain boundaries (intergrain) contributions in transport properties of the material.

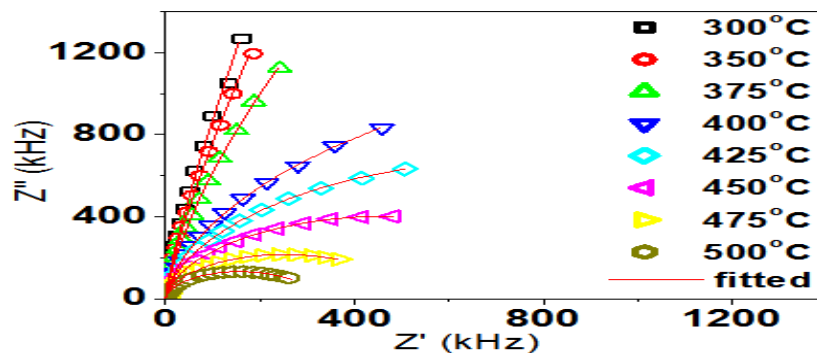


**Fig. 2.  $Z''$  versus  $Z'$  plots of  $\text{Ba}_3\text{Sr}_2\text{LaTi}_3\text{V}_7\text{O}_{30}$  at different temperature.**

Fig. 2 shows the temperature dependence Nyquist Plots (fitted complex impedance spectrum) of BSLTV measured at some selected temperatures (300–500°C) and frequencies. The appeared arc tends to trace a semicircle at higher temperature, but at lower temperatures, the departure of the curves from x-axis indicates that the compound seems to be more insulating at these temperatures. The single semicircular arcs observed at high temperature in the Nyquist plot of this compound indicate that the electrical response is mainly due to the grain effect.

**3.3 Modulus Spectrum study:**

The complex electric modulus formalism plays an important role in discriminating electrode polarization from grain boundary conduction process. The study of modulus spectrum is particularly useful for separating components with similar resistance but having different capacitance. In polycrystalline materials, impedance formalism emphasizes grain boundary conduction process, while bulk effects on frequency domain would dominate in the electric modulus formalism.

Fig. 3 shows the complex modulus spectrum ( $M'$  versus  $M''$ ) of BSLTV at selected temperatures. The modulus plane shows two merged and deformed semicircles at high temperatures. The low frequency semicircle is considered due to the grain boundary (blocking core) whereas the high frequency semicircle depicts the bulk effect. The appearance of two merged semicircles at a particular temperature indicates that the two capacitances (grain and grain boundary) are not nearly equal to each other.

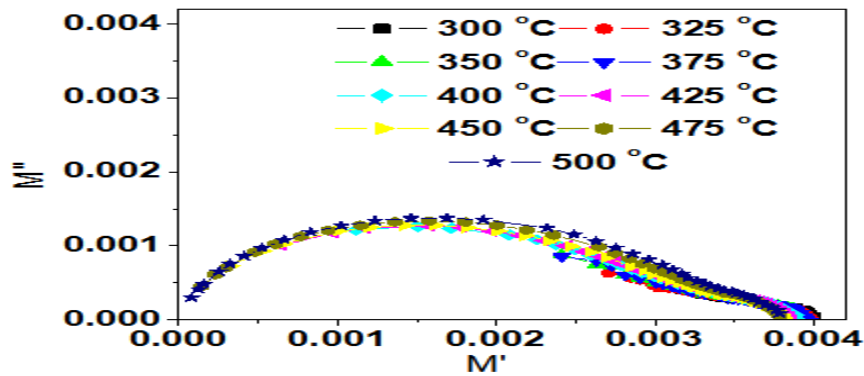


Fig.3.  $M''$  versus  $M'$  plots of  $Ba_3Sr_2LaTi_3V_7O_{30}$  at different temperature.

The merging of the curves indicates the temperature independence nature of capacitance which may be associated with non-ferroelectric regions [15].

**3.4. Comparison of relaxation process in impedance and Modulus loss spectra:**

The frequency variation of  $Z''$  and  $M''$  for the BSLTV compound is as shown in Fig.4 at two different temperatures.

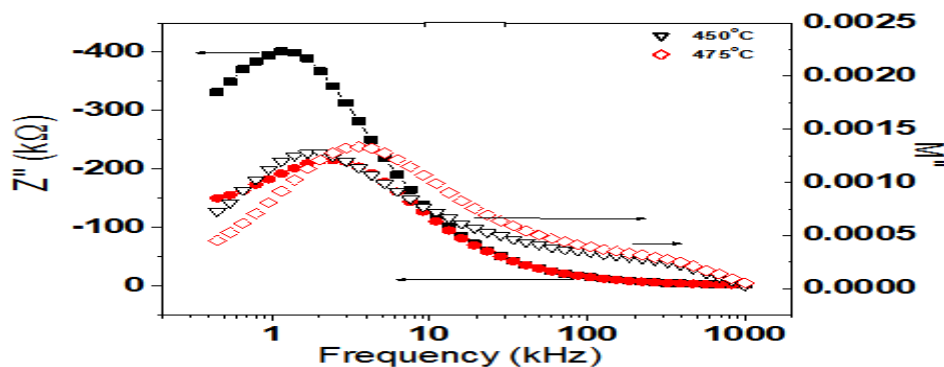


Fig.4. Frequency response of  $Z''$  and  $M''$  of  $Ba_3Sr_2LaTi_3V_7O_{30}$  at three different temperatures

In these plots two subsequent peaks are observed at two different frequencies which confirm that the curves of two data do not collapse to a single curve. This indicates two relaxation processes; first one in  $Z''$  vs. frequency corresponds to grain boundary relaxation and second one in  $M''$  vs frequency corresponds to bulk relaxation. This may be due to the fact that the impedance loss spectra ( $Z''$  vs. Frequency) represent the non-localized conduction phenomena whereas imaginary modulus spectra ( $M''$  vs. Frequency) represent the localized conduction in polycrystalline sample. In addition to the above physical mechanisms, there is also a finite probability of ion diffusion from grain boundary to grain, introducing a polarization relaxation resulting in stretching of conductivity response [16].

### 3.5. Conductivity study

Fig. 5 shows the variation of  $\sigma_{ac}$  with inverse of absolute temperature ( $10^3/T$ ) of BSLTV at different frequencies. The plot shows dispersion in ac conductivity at low temperatures and at low frequencies. But with increase in temperature, a relative increase in low frequency plateau region is observed. The nature of variation of the curve over a wide temperature range supports the thermally activated transport properties of the material obeying Arrhenius equation:  $\sigma_{ac} = \sigma_0 \exp(-E_a/K_B T)$ , where the symbols have their usual meanings. It is observed that the ac conductivity of the material increases with rise in temperature, and shows the negative temperature coefficient of resistance behavior [17].

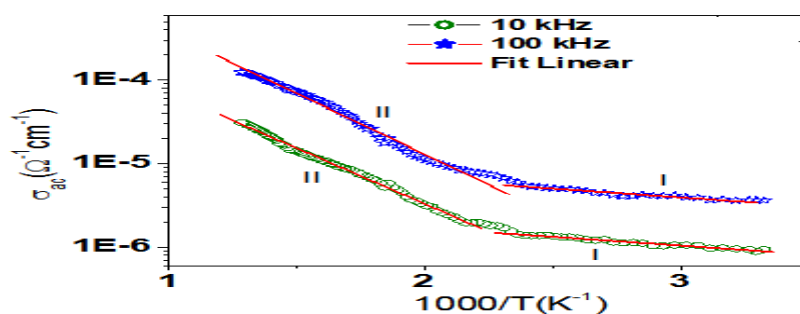


Fig. 5. Variation of  $\sigma_{ac}$  with inverse temperature at 10 and 100 kHz of  $Ba_3Sr_2LaTi_3V_7O_{30}$

The estimated value of activation energy of the compound at 10 and 100 kHz is found to be 0.0418eV, 0.2653eV and 0.0419eV, 0.2895eV in the para and ferroelectric regions (region I and II) respectively. The different values of activation energy in different regions indicates the presence of different conduction mechanism in different regions

## IV. CONCLUSIONS

From the XRD pattern, formation of single-phase orthorhombic crystal structure is observed at room temperature. Impedance spectroscopy is used to characterize the electrical properties of the material which informs the electrical response is mainly due to the grain effect. The different activation energy of the compound observed in different region indicates the presence of different conduction mechanism.

## REFERENCES

- [1] B. Jaffe, W. R. Cook and H. Jaffe, "Piezoelectric Ceramics," Academic Press, London, 1971.
- [2] K. Uchino, "Piezoelectric Actuators and Ultrasonic Motors," Kluwer Academics, Boston, 1997.
- [3] R. R. Neurgaonkar, M. H. Kalisher, T. C. Lim, E. J. Staples and K. L. Keester, "Czoehralski Single Crystal Growth of  $Sr_{0.61}Ba_{0.39}Nb_2O_6$  for Surface Acoustic Wave Applications," *Materials Research Bulletin*, Vol. 15, No. 9, 1980, pp. 1235-1240. doi:10.1016/0025-5408(80)90025-2
- [4] W. Sakamoto, Y.-S. Horie, T. Yogo and S.-I. Hirano, "Synthesis and Properties of Highly Oriented (Sr, Ba)(Nb, Ta) $2O_6$  Thin Films by Chemical Solution Deposition," *Japanese Journal of Applied Physics*, Vol. 40, 2001, pp. 5599-5604. doi:10.1143/JJAP.40.5599
- [5] P. Ganguly and A. K. Jha, "Investigations of Dielectric, Pyroelectric and Electrical Properties of  $Ba_5SmTi_3Nb_7O_{30}$  Ferroelectric Ceramic," *Journal of Alloys and Compounds*, Vol. 484, No. 1-2, 2009, pp. 40-44. doi:10.1016/j.jallcom.2009.05.034
- [6] M. R. Ranga Raju, R. N. P. Choudhary and S. Ram, "Dielectric and Electrical Properties of  $Sr_5EuCr_3Nb_7O_{30}$  Nanoceramics Prepared Using a Novel Chemical Route," *Physica Status Solidi (b)*, Vol. 239, No. 2, 2003, pp. 480-489. doi:10.1002/pssb.200301832
- [7] P. V. Bijumon, V. Kohli, Om Parkash, M. R. Varma and M. T. Sebastian, "Dielectric Properties of  $Ba_5MTi_3A_7O_{30}$  [M = Ce, Pr, Nd, Sm, Gd, Dy and Bi; A = Nb, Ta] Ceramics," *Materials Science and Engineering: B*, Vol. 113, No. 1, 2004, pp. 13-18. doi:10.1016/j.mseb.2004.05.023
- [8] M. R. Ranga Raju and R. N. P. Choudhary, "Structural, Dielectric and Electrical Properties of  $Sr_5RTi_3Nb_7O_{30}$  (R = Gd and Dy) Ceramics," *Materials Letters*, Vol. 57, No. 19, 2003, pp. 2980-2987. doi:10.1016/S0167-577X(02)01408-8

- [9] H. Zhang, Z. Q. Liu, C. L. Diao R. Z. Yuan and L. Fang, "Structural and Dielectric Properties of Sr<sub>4</sub>Ln<sub>2</sub>Ti<sub>4</sub>Ta<sub>6</sub>O<sub>30</sub> (Ln = Nd and Sm) Ceramics," *Materials Letters*, Vol. 59, No. 21, 2005, pp. 2634-2637. doi:10.1016/j.matlet.2005.04.006
- [10] X. H. Zheng and X. H. Zhou, "Crystal Structure and Dielectric Properties of La<sup>3+</sup> Substituted Ba<sub>5</sub>LaTi<sub>3</sub>Ta<sub>7</sub>O<sub>30</sub> Ceramics," *Journal of Materials Science: Materials in Electronics*, Vol. 17, No. 12, 2006, pp. 987-991. doi:10.1007/s10854-006-9007-5
- [11] L. Fang, H. Zhang, J. F. Yang, X. K. Hong and F. C. Meng, "Preparation, Characterization and Dielectric Properties of Sr<sub>5</sub>LnTi<sub>3</sub>Ta<sub>7</sub>O<sub>30</sub> (Ln = La, Nd) Ceramics," *Journal of Materials Science: Materials in Electronics*, Vol. 15, No. 6, 2004, pp. 355-357. doi:10.1023/B:JMSE.0000025677.53710.c8
- [12] E. Wu, POWD, An Interactive Powder Diffraction Data Interpretation and Indexing Program, Version 2.1 (School of Physical Sciences, Flinders University South Bedford Park), SA 5042 Australia.
- [13] Klug, H.P.; Alexander, L.E.; *X-ray Diffraction Procedures for Polycrystalline and Amorphous Materials*, (Wiley-Interscience, New York, 1974).
- [14] J.R. MacDonald "Impedance Spectroscopy", Wiley, New York, 1987.
- [15] D. C. Sinclair, A. R. West, *J. Mater. Sci.* **29** (23) (1994) 6061.
- [16] S.R.Elliot, *Journal of Non-Crystalline Solids* **172-174** (1994) 1343.
- [17] K. Sambasiva Rao, P. Murali Krishna, D. Madhava Prasad, Joon-Hyung Lee, Jin- Soo Kim, *J. Alloys and compounds* **464**,497 (2008)